Bulk density measurement and coating porosity calculation for coated paper samples

Cathy J. Ridgway and Patrick A.C. Gane

SUMMARY

During mercury intrusion at low pressure into uncoated and pigment-coated papers, irreproducible large pore volumes are frequently recorded which prevent detailed determination of total composite porosity by mercury porosimetry alone. A novel occlusion-correction procedure is reported here, in which the absorption volume of hexadecane into the void structures and its displacement by the skeletal structures are combined with the mercury intrusion data to allow the coating and the substrate to be separately assessed. This may be achieved either directly, in the case of a non-permeable substrate, or by scaling the intrusion into the uncoated permeable substrate to that of the coated substrate intrusion curve. This is then scaled to an absolute porosity and bulk volume of the coated sample. The values so derived are compared to those obtained by the traditional method of approximating the intrusion volume into the coating and to the coating applied to an aluminium foil substrate. A method for estimating coating coverage derived from these analyses is described.

Keywords: Porosimetry, mercury intrusion, laminate structures, coated paper porosity, fibrous materials structure, paper structure, coating coverage

---

Address of Authors: Paper and Pigment Systems Research, Omya AG, CH 4665 Oftringen, Switzerland.

Introduction

Mercury porosimetry of coated and uncoated permeable fibrous and non-permeable laminate papers is known to be inherently limited in its application due to observed inconsistencies related to the initial mercury intrusion under low pressure conditions. Despite these drawbacks, previous workers, for example, Donigian *et al*. (Donigian *et al.* 1997) and Johnson *et al*. (Johnson *et al.* 1999) have analysed coating pore structure in isolation from the base paper. This was achieved by removing the low-pressure data, and perhaps even the transition region beyond. Whilst this is accepted practice for studying a coating layer, it prevents analysis of the inevitable modifications of the base paper brought about by applying the coating. Such modifications can include structural changes in the paper, and surface pore filling by the fine coating pigment components.

Mercury intrusion data experimentation for a synthetic plastic mineral-filled laminate, Synteape™, and for three natural coated and uncoated papers, are taken as examples to illustrate the problem. The experimental lack of reproducibility is clearly demonstrated in that there is often a variation in the results associated with large void features. The irreproducibilities, however, are confined to the low pressure intrusion region and are a combination of effects arising from the sample preparation, the method of introduction into the sample chamber of the penetrometer, and the occlusion of mercury from surface and edge features that do not form part of the porous structure under analysis. The random occurrence of such surface-related mercury occlusions in repeated sampling of the same material can account for the high variability in the low pressure measurements even though every precaution may have been taken to make sample preparation reproducible.

The use of a filled plastic laminate in this study provides a substrate that has a defined non-permeable microroughness and so acts to hold an applied coating layer on the surface without any associated modification of the substrate structure. The coating can then be compared to a similar one applied to a natural fibrous substrate to give information about surface pore filling of a typical base paper. The laminate in question here has voids within its laminar structure, but, unlike natural fibrous base papers, these voids have little or no connectivity.

A method has been developed which combines the data from mercury intrusion with those of the absorption of an inert liquid. The choice of liquid is important as many coating structures contain latex binders which are diffusionally absorptive and may swell. Rousu *et al*. (Rousu *et al.* 2001) showed that common latices are most sensitive to slightly polar liquids, so it is important to use a non-polar aliphatic when absorbing into coating structures. The skeletal volume and the absorption volume of coated and uncoated samples can therefore be determined independently from that of mercury intrusion by using immersion in the inert liquid, Archimedean displacement and supersource wicking. These values are then used to impose boundary conditions on the mercury intrusion at low pressure and to modify the fully intruded volumes of coated and uncoated papers. It is then possible to determine coating porosity characteristics that are independent of the substrate, the level of coating-substrate interaction (pore filling etc.) and substrate porosity.

™ Synteape is a product name of Arjo Wiggins

MERCURY POROSIMETRY OF SHEET-LIKE MATERIALS

Sample Preparation

To minimise the effects from sample surface contact with the penetrometer wall during mercury intrusion, which are typical of strongly two-dimensionally biased samples, the following new method has been developed.

A strip of the sample has 5 mm diameter holes punched out of it, situated regularly along its centre line. The perforated strip is then threaded onto a piece of metal wire (stainless steel chosen to avoid amalgam effects with the mercury) which is wound into a spiral of such an outer diameter that it can be placed, without touching the wall, in the penetrometer, Figure 1. The sample weight, 0.2 g, fits well into a 15 cm^3 penetrometer with a 0.392 cm^3 stem volume.

This procedure prevents the formation of pockets that might be unintrudable at low pressure. The perforation voids are automatically incorporated into the bulk density calculation.

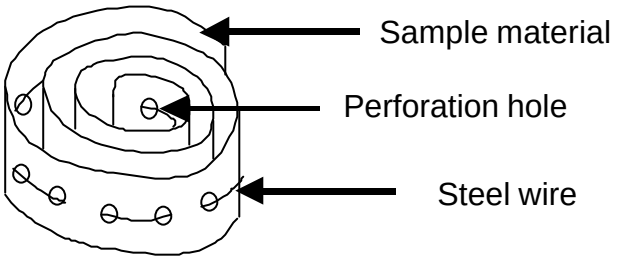

Figure 1. Sample preparation using a scrolled forming wire.

Mercury intrusion measurements were made using a Micromeritics Autopore III mercury porosimeter. The maximum applied pressure of mercury was 414 MPa, equivalent to a Laplace throat diameter of 0.004 μm. The equilibration time at each of the increasing applied pressures of mercury was set to 60 seconds. The mercury intrusion measurements were corrected, using the software Pore-Comp[1], for the compression of mercury, expansion of the penetrometer and compressibility of the solid phase of the sample. The following equation from Gane *et al.* (Gane *et al*. 1996) was used:

$$V_{\text{int}} = V_{\text{obs}} - dV_{\text{blank}} + \left[0.175(V^1_{\text{bulk}})\log_{10}\left(1+\frac{P}{1820}\right)\right] - V^1_{\text{bulk}}(1-\Phi^1)\left(1-\exp\left[\frac{(P^1-P)}{M_{\text{ss}}}\right]\right) \quad (1)$$

in which V_{int} is the volume of intrusion into the sample, V_{obs} the intruded mercury volume reading, dV_{blank} the change in the blank run volume reading, V^1_{bulk} the sample bulk volume at atmospheric pressure, P the applied pressure, Φ^1 the porosity at

[1] Pore-Comp is a software program developed by the Environmental and Fluids Modelling Group, University of Plymouth, PL4 8AA, U.K.

atmospheric pressure, P^1 the atmospheric pressure and M_{ss} the bulk modulus of the solid sample.

Laminate Materials - synthetic paper (Synteape)

Figure 2 shows an electron micrograph of Synteape in cross-section. Voids occur at the exposed cut edge, but they are not interconnected to the other voids within the bulk structure. Such edge voids create the likely conditions for mercury occlusion, in a way similar to that expected for random surface fibres, as described below. It is therefore informative as a comparative model when making intrusion analyses.

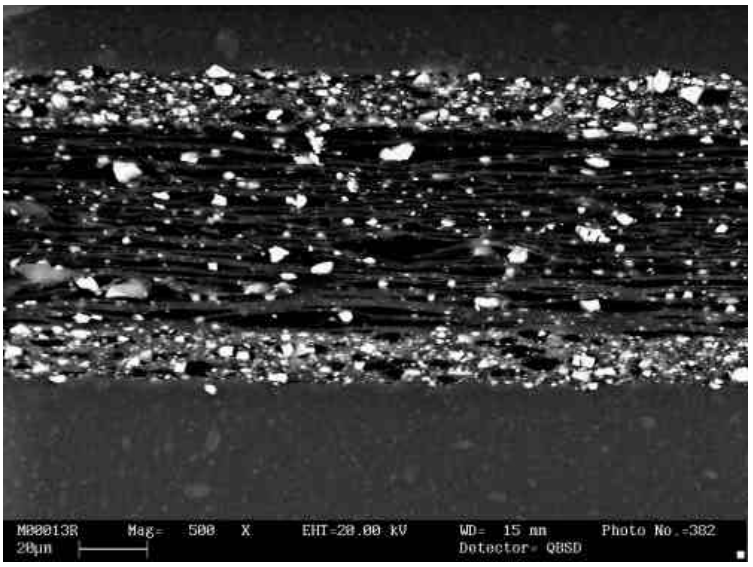

Figure 2. Scanning electron microscope image of a cross-section of Synteape - the highly filled impermeable outer layers contrast with the lamellar bulk structure.

Figure 3 shows five independent Pore-Comp corrected intrusion runs for samples cut from the same Synteape sheet. The dimensions and direction of cut were kept constant, and the same measurement conditions were used. But, despite the precautions taken in sample preparation, it is clear that there is still some residual low pressure measurement variation. The actual shapes of the intrusion curves beyond the low pressure region are almost identical; the differences occur in the initial part of the intrusion curve, from the start at evacution to the last point taken in the low pressure port, 0.138 MPa.

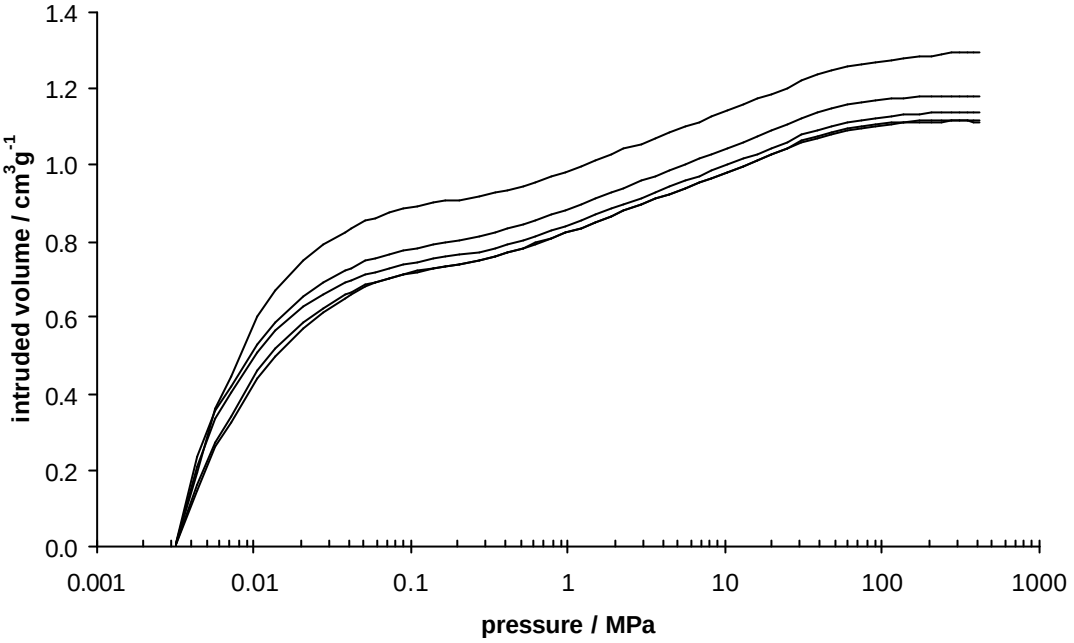

Figure 3. Mercury intrusion curves for Synteape showing low pressure penetration variations leading to a range of irreproducible porosity values.

Uncoated and Coated Fibrous Paper

A similar effect is also seen with mercury intrusion curves for fibrous paper samples. Figure 4 shows results for a typical light weight coated (LWC) base paper, a bulky precipitated carbonate-filled copy paper and a European two-side coated multi-coated woodfree grade.

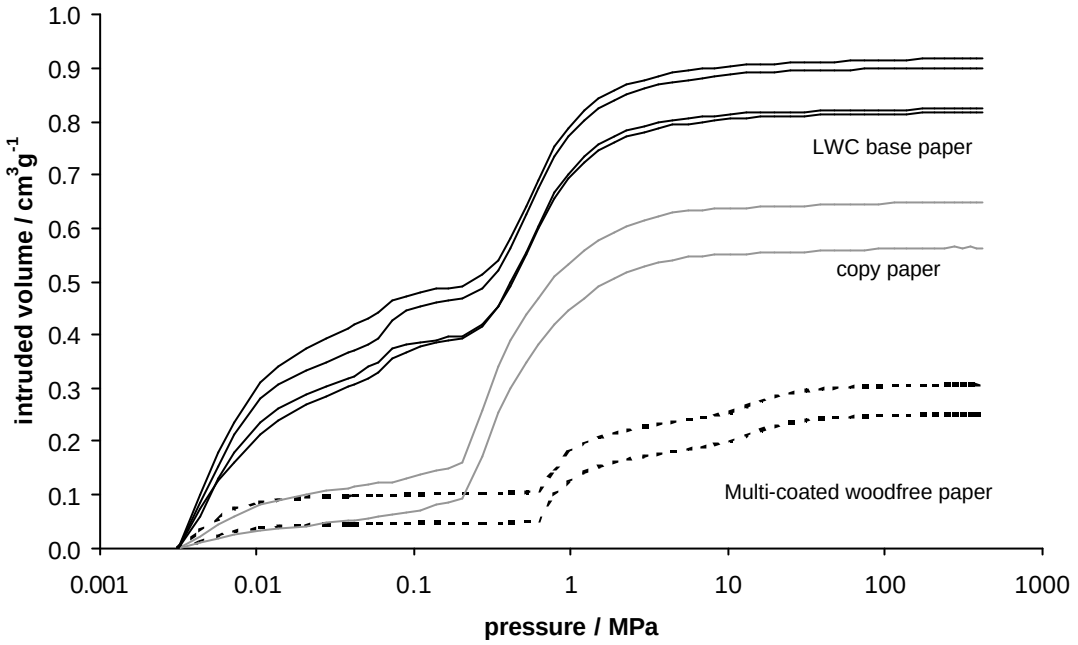

Figure 4. Mercury intrusion curves for different paper types, each showing the irreproducibility at low intrusion pressure.

The type of mercury occlusion effect thought to be responsible for these variations in fibrous paper is shown schematically for the case of a protruding fibre in Figure 5.

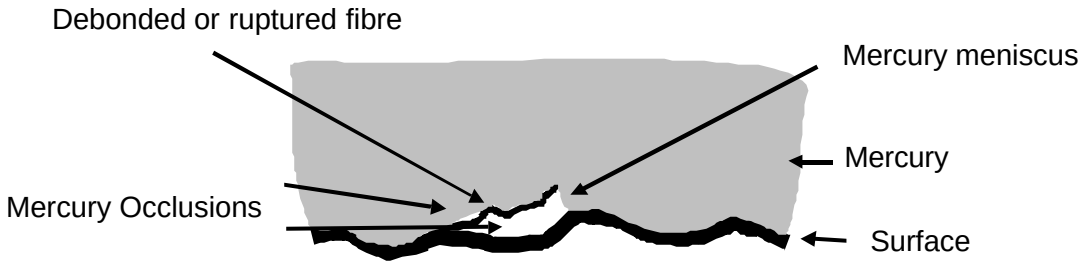

Figure 5. Schematic of possible low pressure mercury occlusion from sample surface or edge features.

A similar effect can be envisaged where an edge irregularity occurs on an otherwise regular sample contributing surface roughness which acts to occlude mercury. These features are clearly not part of the internal porous structure, but are randomly distributed.

Corrections for Occlusion - comparison with liquid absorption for laminate, coated and uncoated fibrous substrates

Firstly, a separate measurement of the accessible porous volume for the sample needs to be made so that the occlusions during the initial stage of the mercury intrusion experiment are not included as part of the sample volume. This is achieved in the case of paper readily by absorbing hexadecane, which is known to fill effectively the entire

available void volume of a pigmented porous structure (Gane *et al.* 2000) and is assumed here to be representative of the volume available for mercury intrusion. Furthermore, interaction with latex, which occurs as a component of many coatings, is largely avoided. A number of paper tests that are based on oil absorption make the same assumption (TAPPI Press 1998).

The sample is weighed initially, then hung, dipping into a dish of hexadecane, in a wicking configuration with its planar surface held vertically. The weight loss from the dish is continually recorded in a draught-free environment. When the recorded weight is constant, indicative of saturation, the sample is weighed again. Dividing the weight difference by the density of the hexadecane gives the volume intruded into the sample, and hence the volume per gram. The average from five such samplings was calculated. Then, placing a known weight of absorption-saturated sample into a previously determined volume of hexadecane and noting the volume difference gives the skeletal volume per unit weight of the original sample. This is best performed using a pycnometer.

In the case of Synteape, the hexadecane penetrated only into the edge pores and not through the impermeable surface of the sample. Absorption must therefore be allowed to occur into all four edges of such a sample because the material is non-isotropic and has low connectivity. The volume absorbed is equal to the volume of mercury that would have been intruded by the start of the higher pressure intrusion curve (i.e. at a pressure of 0.138 MPa).

The absorption volume of hexadecane can then be used to correct the mercury intrusion curve. Applying this correction to the Synteape curves in Figure 3 gives the curves shown in Figure 6, which, at higher pressures, are now shown to be virtually coincident, indicating clearly that the internal porous structure is very uniform and that the earlier irreproducible intrusion curves are related to surface features only.

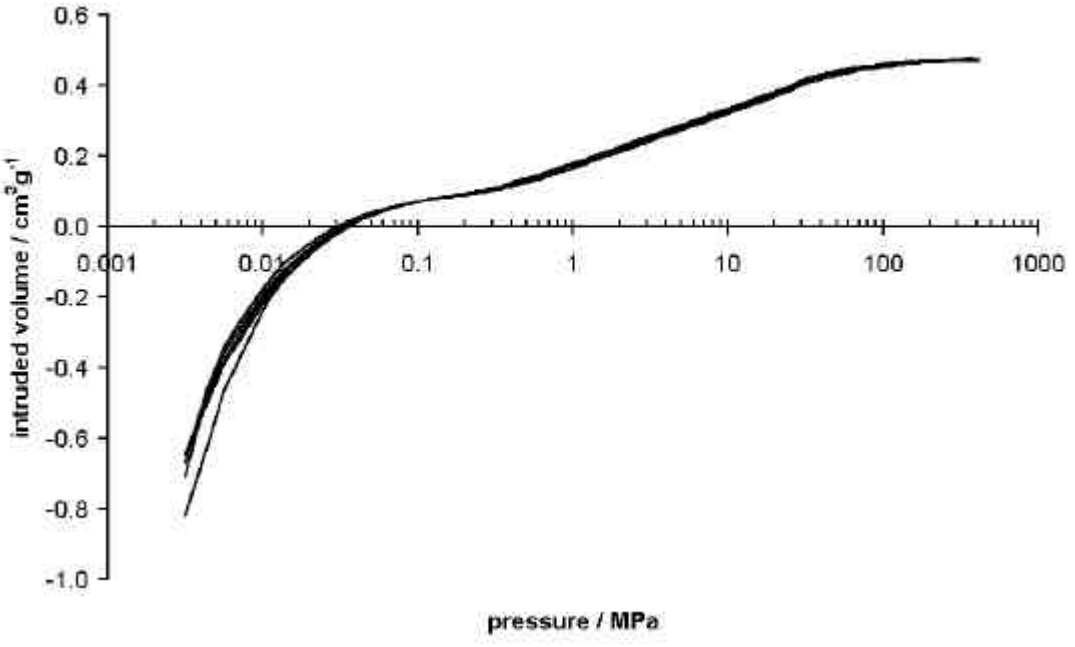

Figure 6. Occlusion-corrected Synteape mercury intrusion curves.

The same procedure was followed for the fibrous paper substrate samples to transform the curves of Figure 4 into those shown in Figure 7. Here also, the main parts of the intrusion curves for the duplicate measurements are now coincident. There is still a slight discrepancy at the start of the two uncoated copy-paper measurements which indicates that the mercury occlusions and associated surface and edge voids in this case need a slightly higher pressure (0.207 MPa) to overcome them, but this does not affect the reproducibility of the curves at higher pressure.

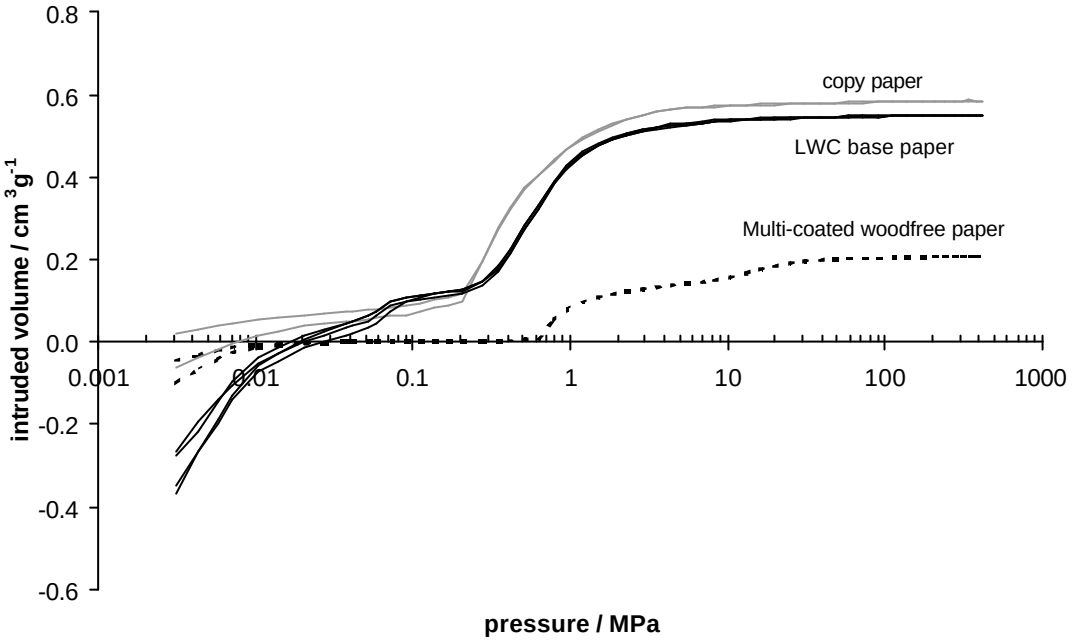

Figure 7. Occlusion-corrected intrusion curves for the three different paper types

Knowing the skeletal density, as obtained by pycnometry, the true bulk volume, V_{sample}, can be calculated as the sum of skeletal volume (displacement), $V_{\text{displaced by saturated sample}}$, and void volume (absorption), $V_{\text{absorbed into sample}}$. The porosity is then calculated as

$$f = \frac{V_{\text{absorbed into sample}}}{V_{\text{sample}}} \tag{2}$$

where

$$V_{\text{sample}} = V_{\text{absorbed into sample}} + V_{\text{displaced by saturated sample}} \tag{3}$$

This procedure is summarised in the following flow chart, Figure 8.

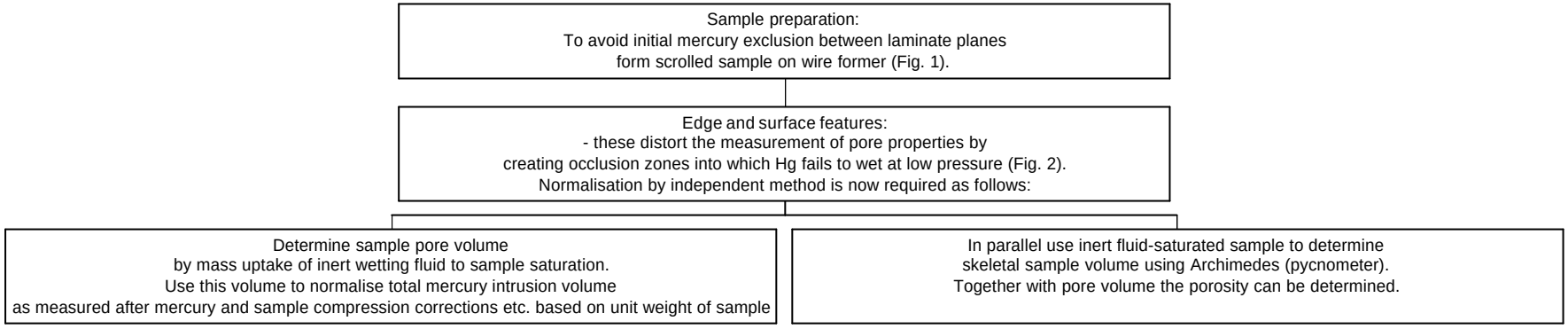

Figure 8. Procedure for determining the true intrusion porosity of laminate and fibrous materials

Separating the Intrusion Curves for Coatings and Substrate

The occlusion-corrected mercury intrusion curves for a substrate, such as an uncoated base paper or the uncoated laminate, can be subtracted from those for the coated substrate to enable the intrusion into the coating alone to be determined. In the case of a non-permeable substrate, or a non-connected external voidage laminate, such as Synteape, the only correction necessary to allow subtraction of substrate from coating-plus-substrate is that of occlusion, as has just been described. This case is, therefore, not discussed further here, but is exemplified later by the use of coating onto an aluminium foil substrate. However, a natural fibrous substrate or one with penetrable surface porosity cannot be treated in this simple way.

In this section, a series of one-side single-coated woodfree papers is studied. This more complicated case of a porous substrate requires that the effects of coating penetration and substrate change as a result of coating be taken into account. Without detailed knowledge of the base paper change during coating it would not normally be possible to determine the overall composite porous behaviour. However, deviation from a simple additive analysis, i.e. deviation from a representation of coating plus unchanged uncoated base paper only, gives information about the coating penetration of surface voids and the changes in base paper structure.

The base paper weight was 77 gm^{-2}. The coating pigments used were 100 % ground calcium carbonates of different mean particle sizes and particle size distributions, Table 1. The coating colours contained only a styrene butadiene latex as binder. The binder level was kept constant at 12 parts by weight based on pigment throughout the series. The colours were applied on a laboratory Helicoater[2] using a short dwell coating head at 12 gm^{-2} coat weight with an application speed of 1 000 $mmin^{-1}$.

Pigment	Specific surface area / m^2g^{-1}	Particles < 2 µm / w/w%	Particles < 1 µm / w/w%	Median particle size by weight (d_{50}) / µm
Hydrocarb 90 (HC90)	12.5	90	64	0.7
Setacarb (=Hydrocarb 95) (SC)	19.2	98	90	0.38
Covercarb 75 (CC)	9.0	95	75	0.52

Table 1. Coating pigment data[3].

The methodology described above was applied, performing independent measurements of the total intrudable volume and the skeletal density of both the coated sample and of the uncoated substrate by comparing hexadecane absorption with mercury intrusion. Care is needed in the case of coated samples as the time taken to reach equilibrium for absorption can be significantly longer than for uncoated substrates. The addition of the values for absorbed volume and skeletal volume (by

[2] Helicoater is a product name of Dixon Coaters
[3] Hydrocarb 90, Setacarb (Hydrocarb95) and Covercarb 75 are product names of Omya AG, CH 4665 Oftringen, Switzerland

displacement) will give a value for the bulk volume of the sample according to equation (3).

The initial Pore-Comp corrected mercury intrusion curves give an unrealistically high intrusion volume due to the low pressure intrusion variations and especially the occlusion effect. The curves are therefore translated linearly down the *y* axis until the correct final intrusion volume, determined from the hexadecane absorption, is achieved, Figure 9. The low pressure cut-off point is usually taken to be at 0.138 MPa, the last low pressure analysis point. As was the case for the copy grade paper previously, there remains a small step at the start of the curve from this cut-off point for a fibrous base paper showing that there is some realistic pore intrusion during this initial stage, but the exact intrusion details are not interpretable due to the overlying occlusion effect.

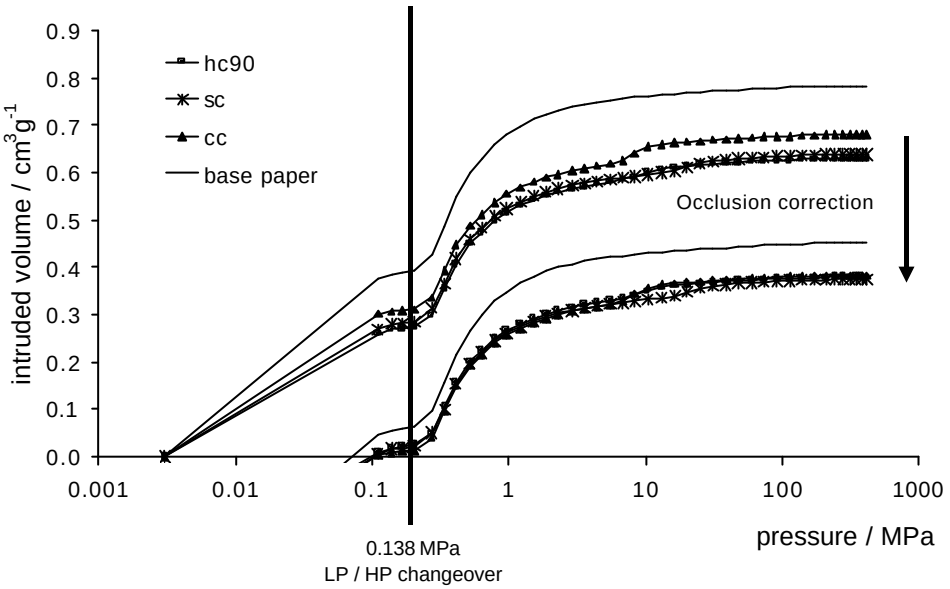

Figure 9. Mercury intrusion curves corrected to volume of hexadecane absorbed - a cut-off point for data acceptance is set at the low pressure (LP) to high pressure (HP) port changeover.

It is well known that paper substrates change during the coating and drying processes, with release of stress, fibre roughening and surface filling of the outermost voids by the pigmented coating (Gane, Hooper 1989), (Gane *et al.* 1991). If the gradients at the start of the individual intrusion curves for both uncoated and coated paper are equal, this suggests that the mercury is intruding initially into the base paper (after overcoming any surface and occlusion effects), and before any intrusion into the coating layer has occurred. The intrusion in this region relates only to the internal large scale structure of the base paper, and so this structure can be taken to have been unaffected by the coating itself. By using a progressive shift function (see Appendix) it is possible to make the uncoated base paper curve lie on top of the coated paper curve from this region up to the pressure where intrusion into the coating becomes apparent. This procedure is assumed valid in the case of uncalendered papers. For calendered coated papers, however, things are more complicated: a strategy for calendering the uncoated base paper under conditions such that the same initial mercury intrusion curve gradient as that of the calendered coated sample would have

to be devised. This calendered base paper could then be considered as the underlying substrate for the independent absorption and intrusion experiments. It is, however, to be expected that the variability using such a method would be greater than in the case of uncalendered coated papers.

In the examples studied here, the gradients are seen to be similar from an intrusion pressure of 0.276 MPa, so this is taken as the starting point for curve fitting. The method developed to correlate the various curves is illustrated for one of the test samples in Figure 10. The squares are the original intrusion data for the uncoated base paper. The curve fitted to these data, using the software package TableCurve 2D[4], is shown by a line joining these points. The mathematical form of the curve is irrelevant to the analysis and simply provides a continuous curve for analytical differentiation, scaling etc. The triangles represent the part of the initial curve of the coated sample which is derived from the gradient correspondence with the uncoated substrate and which is fitted up to the beginning of intrusion into the coating. Next, the progressive shift function $S(x)$ (see Appendix) is determined, which moves the fitted uncoated substrate curve onto that for the fitted coated substrate. This shift function is not a single value but is progressive in x, i.e. a function of the pressure of intrusion. It is then applied to the complete uncoated intrusion curve to provide an extrapolation for the whole of the coated base paper, shown as the dashed line. The function to do this is also conveniently found using TableCurve 2D.

This newly formed coated substrate curve can then be subtracted from the coated sample curve to give the intrusion volume curve for the coating alone. The coating layer curve so derived is for that layer which is independent of the proportion of coating that might have been involved in modifying the base paper, i.e. that part of the coating that does not fill or partially fill the voids in the base paper. In reality, of course, at least part of the coating will have entered the interactional surface voidage of the base paper.

The intruded volume per unit weight thus derived will be dependent, therefore, on coating holdout. The more coating that is lost into the base paper surface, the lower will be the observed independent intrusion per unit weight of coating. This leads to a lower pore volume than the coat weight might normally suggest. This intrusion volume associated with coating free of penetration into the base paper can be back-correlated with a simple intrusion volume obtained by truncating the intrusion curve at the point of coating intrusion, as has been done by previous workers (Johnson *et al.* 1999). The difference between the two values is then a measure of the extent to which the coating has brought about surface modification of the base paper. For a laminate film, such as Synteape, the two values will be approximately equal, i.e. the coating coverage is 100 %. For a fibrous substrate the density of the coating derived by the two methods may differ by up to 50 %, suggesting a potential of 50 % coverage by volume. This issue will be pursued later in the summary of the experimental data.

[4] TableCurve 2D is a software program of SPSS Inc., 444 North Michigan Avenue, Chicago, IL 60611, USA

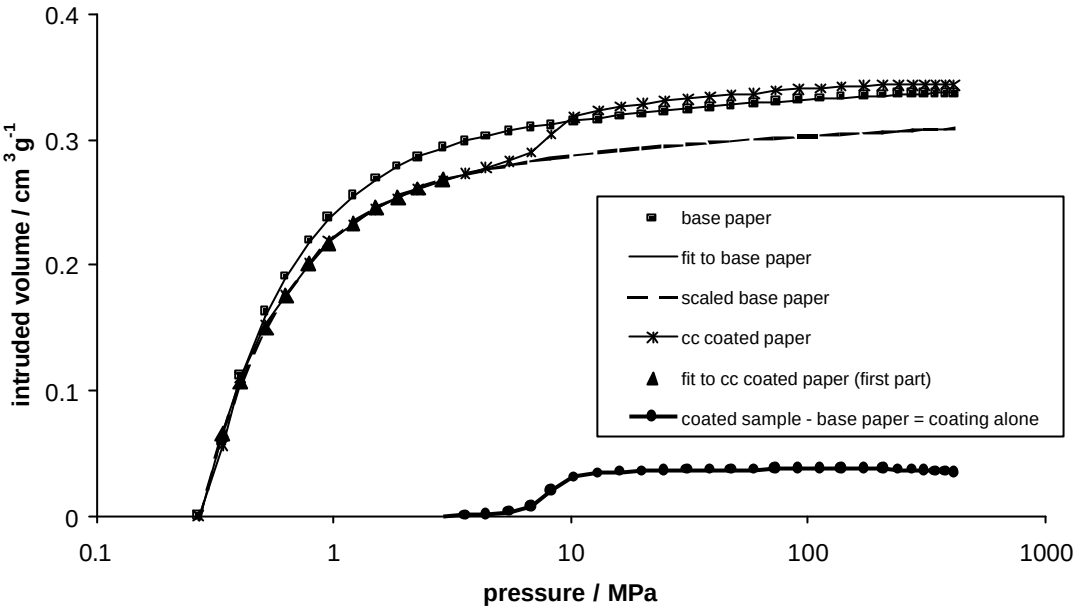

Figure 10. Occlusion-corrected, uncoated base paper intrusion, fitted and shifted to represent the coated base paper intrusion curve as used to calculate the mercury intrusion into the coating by extrapolation and subtraction.

The abscissa values of the intrusion curves can alternatively be expressed in terms of pore diameter, derived from the equivalent Laplace pore intrusion pressure; this will be the preferred parameter in the following sections.

Determining the Porosity after Occlusion Correction

If the weight of coating is known, the intruded volume per unit weight of coating can be calculated (Lepoutre 1978), (Lepoutre, Rezanovich 1977), (Zhang *et al.* 2001), but not yet an actual porosity value. This can be determined, however, as the total intrusion volume into the sample is known from the hexadecane measurement. The mercury intrusion volume into the coating is also known from the calculation in the previous section, $V_{\text{coating intrusion}}$. The intrusion volume into the coated base paper alone, $V_{\text{Hg intrusion into coated base}}$, can now be calculated from the extrapolated coated base paper curve by,

$$V_{\text{Hg intrusion into coated base}} = (V_{\text{sample intrusion}} - V_{\text{coating intrusion}}) \tag{4}$$

where the value of $V_{\text{Hg intrusion into coated base}}$, through the other parameters in equation (4), is already corrected for occlusions, and represents the state of the base paper underneath the coating layer which would exist if the coating had perfect holdout, i.e. if none of the coating had entered the surface voidage of the base paper.

The skeletal volume of the coated base paper, $V_{\text{skeletal coated base}}$, can now be found by applying an appropriate scaling factor, S, to the bulk volume of the uncoated base paper sample, $V_{\text{uncoated base}}$, as measured by hexadecane volume absorption and

displacement after saturation (equation (3)), using the known mercury intrusion occlusion-corrected volumes of the coated and uncoated base papers:

$$V_{\text{skeletal coated base}} = S.V_{\text{uncoated base}} - V_{\text{Hg intrusion into coated base}} \quad (5)$$

where

$$S = \frac{V_{\text{Hg intrusion into coated base}}}{V_{\text{Hg intrusion into uncoated base}}} \quad (6)$$

and

$$V_{\text{Hg intrusion into uncoated base}} = V_{\text{hexadecane absorbed into uncoated base}} \quad (7)$$

S represents the volume scaling, and hence weight scaling, applied to the uncoated base paper so that it represents the mercury intrusion into the actual coated base paper under the coating layer. This observation is important, since all the intrusion data are given as volume intruded per unit weight of relevant sample. Therefore, all relevant weights must refer to the weight of uncoated base paper, coating and coated base respectively, i.e. that weight fraction of the uncoated base paper which represents the weight of coated base paper unfilled by coating penetration. This simply re-states the case described earlier regarding coating holdout, but, here, from the perspective of the base paper.

The mass of the coated sample, m_{sample}, is known, and so, knowing the ratio of coating mass to base paper mass, $m_{\text{coating}}/m_{\text{base}}$, the independent values of m_{coating} and m_{base} can be determined for the individual samples under test. The volume of the coated base, $V_{\text{coated base}}$, is thus calculated from the skeletal volume of the coated base paper plus the intruded volume into the coated base paper. Thus, the volume of the coating itself, free from base paper surface voids, V_{coating}, is the total sample volume, V_{sample}, less the volume of the coated base.

The porosity can now be calculated, as in equation (1), as the volume of mercury intruded into the coating over the total volume of the coating, which now includes all the necessary occlusion corrections.

$$f = \frac{V_{\text{Hg intrusion into coating}}}{V_{\text{coating}}} \quad (8)$$

RESULTS - porous structure analysis, coating-substrate deconvolution, determination of coating coverage and associated porosity

The occlusion correction and subtraction methods above have been used for the analysis of the three samples in the study series. The relevant fitting functions are shown in the Appendix. The resulting coating intrusion curves are shown in Figure 11, the coated base intrusion curves are shown in Figure 12 and the porosity calculations are shown in Table 2.

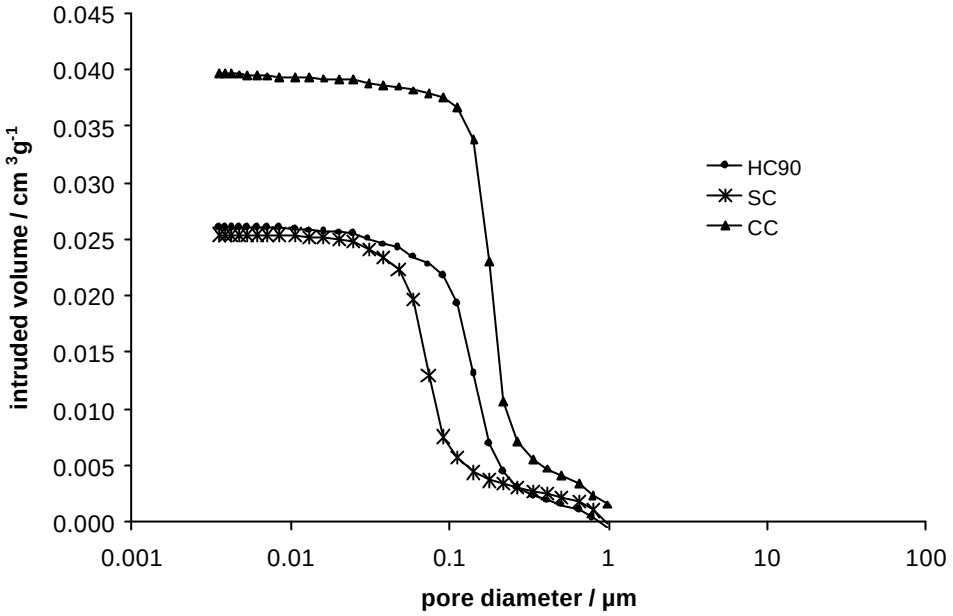

Figure 11. The separated coating intrusion curves.

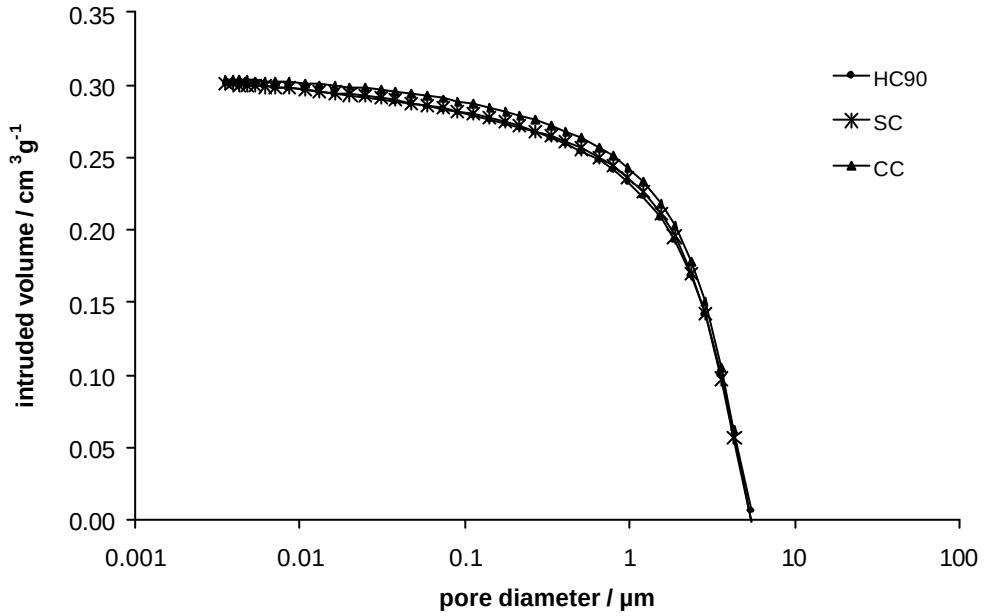

Figure 12. The separated coated substrate intrusion curves, i.e. the base papers underneath the coatings.

Progressive shift function		HC90	SC	CC	Base
m_{sample}	/ g	0.3710	0.3500	0.3290	
$m_{coating}$	/ g	0.0498	0.0470	0.0442	
$m_{uncoated\ base}$	/ g	0.3212	0.3030	0.2848	
$V_{Hg\ intrusion\ into\ coating}$	/ cm^3g^{-1}	0.0260	0.0250	0.0380	
$V_{oil\ absorption\ into\ sample}$	/ cm^3g^{-1}	0.3913	0.3862	0.4005	0.5120
$V_{skeletal\ sample}$	/ cm^3g^{-1}	0.6991	0.6784	0.7382	0.7602
V_{sample}	/ cm^3g^{-1}	1.0904	1.0646	1.1387	1.2722
$V_{Hg\ intrusion\ into\ coated\ base}$	/ cm^3	0.1355	0.1264	0.1193	
$V_{skeletal\ coated\ base}$	/ cm^3	0.2012	0.1877	0.1771	
$V_{coated\ base}$	/ cm^3	0.3367	0.3141	0.2963	
$V_{coating}$	/ cm^3	0.0678	0.0585	0.0783	
Porosity, F_S	/ %	14.23	14.96	15.96	
Traditional straight line approximation					
$V_{Hg\ intrusion\ into\ coating}$	/ cm^3g^{-1}	0.0590	0.0600	0.0720	
Porosity, F_0	/ %	22.29	23.62	22.33	
F_S / F_0		0.64	0.63	0.71	

Table 2. Parameter and porosity values determined by the new correction methods.

The intrusion curves were corrected initially by Pore-Comp, as previously described, to remove the effect of skeletal compression. The most compressive components in the coatings are the latex binder and the surface fibres penetrating into the coating layer. After applying this correction, the volume intruded associated with true open void volume is greatly reduced compared with the void volumes seen when using only compressed pigment structures without the use of binder (Gane *et al.* 2000).

The porosity tends to follow the increasing pigment surface area, from HC90 (the lowest) to SC (the highest). These pigments have broad size distributions; the latex blocking effect will tend to be the greatest for the lowest surface area pigment (HC90). In contrast, the narrow particle size distribution pigment CC shows a deviation from the trend as the reduced number of fine particles leads to a more open structure, even though the specific surface area of the pigment is relatively low.

To confirm the relevance of the porosity values as seen on the fibrous base paper, the pigment (SC) was coated onto aluminium foil and studied in a the same manner as above. As the foil is continuously compressible with a purely elastic modulus, the progressive shift function, to make the uncoated foil lie on top of the substrate curve of the coated foil, can be approximated by manually extrapolating the intrusion curve for the foil alone under that of the coating intrusion - this is an example of the simple case where no coating penetration into the substrate occurs. Subtracting gives the

intrusion into the coating structure. By obtaining the skeletal volume of the aluminium foil it is possible to extract a porosity for the coating, which, at 26 %, can be compared to the value obtained in the case of the fibrous substrate (23 %). The difference can be allocated by the inclusion of the portion that penetrated into the fibrous substrate. The values are therefore reasonable and support the case for the expected reduced coating coverage of fibrous substrates.

If we now compare porosity values, F_{Σ}, obtained by the progressive shift function, with those porosity values, $F_{0,}$, obtained by the assumption that all intrusion beyond the intrusion pressure inflection point of 4.416 MPa in Figure 10 is totally associated with coating, i.e. including that portion filling the base paper voids (Johnson *et al.* 1999), then we see that the porosities F_0 are, as expected, much higher than F_{Σ}. The ratio between these porosities, $F_0/F_{\Sigma,}$ yields, by definition, an effective coverage value, as shown in Table 2. As expected, the narrower size distribution pigment CC gives a greater degree of paper surface coverage, ie. less coating penetration into the base paper surface voids.

SUMMARY AND CONCLUSIONS

A flow diagram to clarify the methods described in this paper is given in Figure 13. It follows the path from the initial correction of the overall intrusion volume, according to independent absorption, through to the separate definition of porosity of the base paper and the coating respectively, ending with a definition of coating coverage.

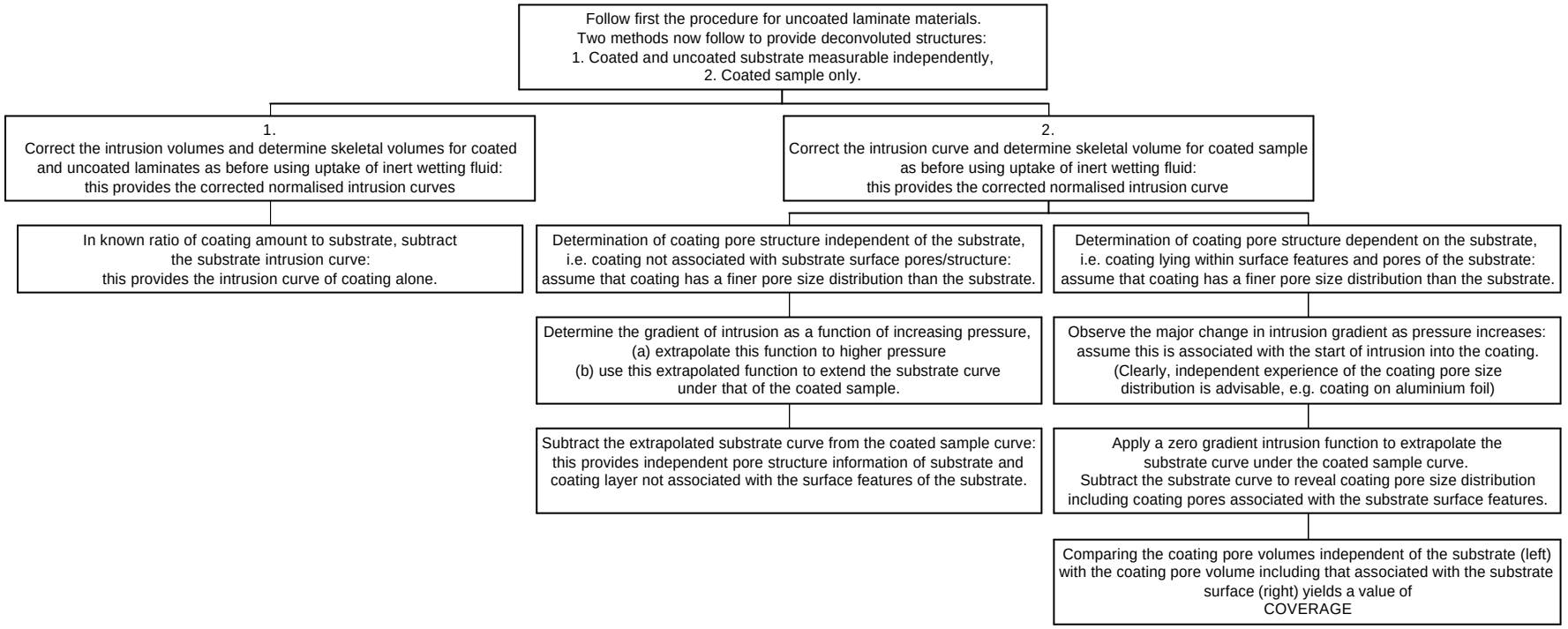

Figure 13. Deconvoluting pore structures of coatings on laminate and fibrous materials, and defining coating coverage, having followed the procedures in Fig. 8.

A phenomenon leading to irreproducibility during mercury intrusion at low pressure into sheet-like materials of either natural fibre or synthetic laminate origin has been defined by the authors as occlusion. It is related to the surface roughness or edge features and not a part of the internal porous structure under investigation. A correction strategy for occlusion has been proposed in which the absorption volumes of hexadecane into the structures of both uncoated substrates and coated samples are compared.

Displacement of hexadecane volume by a saturated sample provides an independent value for the skeletal density, which can be used also to remove occlusion effects which interfere with determinations of skeletal properties as obtained from compression-corrected mercury intrusion data.

Discrimination between a coated base substrate and the coating layer can be further obtained. This is achieved by matching the gradient correspondence of the intrusion curves for uncoated base paper and coated base paper, respectively, applying a progressive shift function to the uncoated substrate intrusion curve to make it coincide with the inital intrusion into the coated sample, assuming that coating pores are finer than those measured during lower pressure intrusion. This procedure gives an extrapolated coated substrate intrusion curve which lies under that of the coated sample. This curve removes the interactional effect of coating on that substrate. Therefore, the volume intruded into that part of the coating that is not associated with base paper surface filling can be determined by difference. Porosity of the coating and of the coated substrate can be distinguished by considering the mass-scaled proportion of the uncoated substrate that would be involved in mercury intrusion into the coated sample. Comparison of the coated substrate porosity with that of the uncoated substrate also provides information on the structural change of that substrate caused by the coating process.

By comparing the ratio of the coating void volume thus obtained, which is unassociated with base paper penetration, with that determined assuming little or no contribution from the base paper in the region of coating pore size intrusion, provides a novel evaluation of coating coverage.

LITERATURE

Donigian, D. W., Ishley, J. N., Wise, K. J. (1997): Coating Pore Structure and Offset Printed Gloss, Tappi Journal, *80*(5), 163.

Gane, P.A.C. and Hooper, J. J. (1989): Coating profilometry: an analysis of coating colour-basepaper interactions, Fundamentals of Papermaking, Transactions of the Ninth Fundamental Research Symposium, 871.

Gane, P. A. C., Hooper, J. J., Baumeister, M. (1991): A Determination of the Influence of Furnish Content on Formation and Basesheet Profile Stability During Coating, Tappi Journal, *74*(9), 193.

Gane, P. A. C., Kettle, J. P., Matthews, G. P., Ridgway, C. J. (1996): Void Space Structure of Compressible Polymer Spheres and Consolidated Calcium Carbonate

Paper-Coating Formulations, Industrial and Engineering Chemistry Research, *35*(5), 1753.

Gane, P.A.C., Schoelkopf, J., Spielmann, D. C., Matthews, G. P., and Ridgway, C. J. (2000): Fluid transport into porous coating structures: some novel findings, Tappi Journal *83*(5), 77.

Johnson, R. W., Abrams, L., Maynard, R. B., Amick, T. J. (1999): Use of mercury porosimetry to characterize pore structure and model end-use properties of coated papers - Part I: Optical and strength properties, Tappi Journal, *82*(1), 239.

Lepoutre, P. (1978): Liquid Absorption and Coating Porosity, Paper Technology and Industry (November), 298.

Lepoutre, P., Rezanovich, A. (1977): Optical Properties and Structure of Clay-Latex Coatings, Tappi Journal, *60*(11), 86.

Rousu, S.M., Gane, P. A. C., and Eklund, D. E. (2001): Influence of coating pigment chemistry and morphology on the chromatographic separation of offset ink constituents, Twelfth Fundamental Research Symposium, Oxford 2001, 1115.

TAPPI Press (1998): "1998-1999 Tappi Test Methods", Tappi Press, Atlanta.

Zhang, Z. R., Wygant, R. W., Lyons, A. V. (2001): A fundamental approach to understand the relationship between top coat structure and paper performance, Tappi Journal, *84*(3), 48.

APPENDIX

The following shows the derived fitting and shift functions used to make the corrections described in the text, where $V(x)$ is the volume intruded per gram of relevant sample into pores of size down to and including a pore diameter of x, and $S(x)$ is the shift function used to move the uncoated base paper intrusion curve to lie on top of that for the coated base paper, so that

$$V_{\text{uncoated substrate}}(x) - S(x) = V_{\text{coated substrate}}(x) . \qquad \text{(A1)}$$

(i) Uncoated base paper

Fitting function for intrusion into the uncoated base paper

$$V(x) = a + bx^2 + cx^3 + dx^{0.5} \qquad \text{(A2)}$$

where a = 0.358204, b = -0.01378, c = 0.001208 and d = -0.06309

(ii) HC 90 coated paper

Fitting function for coated base paper during initial intrusion of coated sample,

$$V(x) = a + bx + cx^{0.5} \quad \text{(A3)}$$

where a = 0.25257, b = -0.06699, c = 0.047486

Shift function,

$$S(x) = a + bx^2 \ln x + cx^3 + dx^{0.5} \ln x \quad \text{(A4)}$$

where a = 0.049633, b = -0.00136, c = 0.00034 and d = -0.01134602

(iii) SC (=HC95) coated paper

Fitting function for coated base paper during initial intrusion of coated sample,

$$V(x) = a + bx^{1.5} + cx^3 \quad \text{(A5)}$$

where a = 0.263373, b = -0.02793, c = 0.000557

Shift function,

$$S(x) = a + bx^2 \ln x + cx^{2.5} + dx^{0.5} \ln x \quad \text{(A6)}$$

where a = 0.050804, b = 0.004608, c = -0.00359 and d = -0.0088314

(iv) Covercarb 75 coated paper

Fitting function for coated base paper during initial intrusion of coated sample,

$$V(x) = a + bx^2 + cx^{2.5} + de^{-x} \quad \text{(A7)}$$

where a = 0.247123, b = -0.02214, c = 0.005893, d = 0.031905

Shift function,

$$S(x) = a + bx^{1.5} \ln x + cx^2 \ln x + dx^3 \quad \text{(A8)}$$

where a = 0.050421, b = -0.00971, c = 0.002618 and d = -0.000369